

Cyclic voltammetry response of coprecipitated $\text{Ni}(\text{OH})_2$ electrode in 5 M KOH solution

Ding Yunchang *, Yuan Jiongliang, Chang Zhaorong

Department of Chemistry, Henan Normal University, Xinxiang 453002, Henan, People's Republic of China

Received 21 October 1996; accepted 22 January 1997

Abstract

A study of the cyclic voltammetry response of a coprecipitated nickel hydroxide electrode in 5 M KOH solution shows that cobalt, manganese and zinc are beneficial additives in practical nickel batteries because they can increase the overpotentials for oxygen evolution reaction at the nickel hydroxide electrodes and decrease redox peak potentials. By contrast, iron and lead are considered harmful to nickel batteries because they can decrease the overpotentials at the nickel hydroxide electrode. On the other hand, the addition of iron is beneficial to the water electrolysis process. Cobalt can act as antidote to iron and lead in batteries. © 1997 Elsevier Science S.A.

Keywords: Cyclic voltammetry; Coprecipitation; Nickel hydroxide electrodes; Cobalt; Manganese; Zinc

1. Introduction

Cobalt, manganese and zinc are usually used as beneficial dopants in nickel battery electrodes [1–10]. By contrast, iron and lead are usually harmful to battery capacity [3], and their contents are therefore strictly controlled during battery production [3–11]. A main reason for limiting the working efficiency of water electrolysis is the higher overpotential of the oxygen evolution reaction (OER), which leads to a higher voltage of the electrolysis cell and excessive assumption of electric energy [9–14]. Nickel is an appropriate positive-electrode material for water electrolysis in alkaline aqueous solution. The reason lies in the fact that a thin film of metal hydroxide is formed on the surface of nickel electrode. In addition, nickel electrodes are often used in batteries and electrosynthesis cells. In order to improve the performance of the electrode, it is necessary to adopt new electrode materials, for example, by doping with transition metal atoms [15]. Since the existence of metal dopants and impurities has a vital effect on the electrochemical performance of the electrode, it is necessary to gain an understanding of the effect of these metal dopants and impurities on the $\text{Ni}(\text{OH})_2$ electrode.

There have been some detailed studies of cyclic voltammetry response of $\text{Ni}(\text{OH})_2$ and $\text{Ni}(\text{OH})_2 + \text{M}(\text{OH})_n$ obtained by chemical coprecipitation in alkaline solutions of various concentration, and the mechanisms have been eluci-

dated to some extent [16,17]. Corrigan [18] studied the OER at electrodes made from nickel and other mixed-metal hydroxides obtained by electrochemical coprecipitation in 1 M KOH aqueous solution. Nevertheless, since 5–8 M KOH solution is widely used in nickel batteries, it is more appropriate to study the cyclic voltammetry response of $\text{Ni}(\text{OH})_2$ electrode in KOH electrolyte of higher concentration.

2. Experimental

2.1. Preparation of the substrate

Nickel foil (1 cm × 1 cm) was used as a substrate. A metal hydroxide thin film that was electrochemically coprecipitated on nickel foil was used as a working electrode.

Prior to use, the foils were degreased by cleaning with detergent and acetone, and then rinsing with water. The foils were next cleaned electrochemically in 5 M KOH solution by passing 5 mA of anodic and cathodic current, each for 30 s. Finally, the foils were stripped in 1 M HCl with an anodic current of 5 mA for 30 s. The cleaned foils were used for deposition after rinsing in distilled water.

2.2. Deposition of thin films

The cleaned nickel foil substrate was placed opposite a platinum foil counter electrode in a rectangular acrylic vessel.

* Corresponding author. Tel.: (0373) 338 3000. Fax: 86 373 3383 145.

Both sides of the nickel foil were used for electrochemical deposition.

The electrolyte solution was made up of 0.05 M $\text{Ni}(\text{NO}_3)_2$, or a mixture of $\text{Ni}(\text{NO}_3)_2$ and one or two of $\text{Co}(\text{NO}_3)_2$, $\text{Mn}(\text{NO}_3)_2$, $\text{Zn}(\text{NO}_3)_2$, $\text{Fe}(\text{NO}_3)_2$ and $\text{Pd}(\text{NO}_3)_2$.

Nickel hydroxide films were prepared by cathodic deposition from 0.05 M $\text{Ni}(\text{NO}_3)_2$ solution. Composite hydroxides were prepared by cathodic deposition from mixed-metal nitrate solutions. 0.05 M nitrate solutions were made up of $\text{Ni}(\text{NO}_3)_2$ and one or two of $\text{Co}(\text{NO}_3)_2$, $\text{Mn}(\text{NO}_3)_2$, $\text{Zn}(\text{NO}_3)_2$, $\text{Fe}(\text{NO}_3)_2$ and $\text{Pd}(\text{NO}_3)_2$. The total concentration of metal ions in the mixed solutions was 0.05 M.

After 1 min in the electrolyte solution, to reduce convection, the metal hydroxide films were deposited by applying a cathodic current of 1 mA for 10 min.

2.3. Instrumentation

A Princeton Applied Research (PAR) Model 363 potentiostat/galvanostat was used to apply current for the deposition procedure, as well as to control the potential during cyclic voltammetry. A 8116A programmable pulse/function generator (HP 8116A) was used to provide the potential wave form for the cyclic voltammetry experiments. Cyclic voltammetry transients were recorded with a YEW 3086 x-y recorder.

2.4. Voltammetry

Cyclic voltammetry experiments of the precipitated films were conducted in 5 M KOH electrolyte.

After deposition, the thin film electrodes were immediately rinsed with distilled water and transferred to a cell that comprised a rectangular vessel constructed from acrylic plastic. The counter electrodes were two platinum foils positioned opposite the working electrode. The working electrode and counter electrodes were immersed in 30 ml of solution. A Hg/HgO reference (5 M KOH) was contacted through a side probe located 2.5 mm from the working electrode.

In cyclic voltammetry experiments, the initial potential was at 0 mV versus Hg/HgO. The potential was first scanned anodically at 10 mV s^{-1} past nickel hydroxide oxidation peak into the oxygen evolution region. The potential was then scanned past the nickel hydroxide reduction peak. The next cycle was then commenced. The potential scan covered a potential range between 0 and 0.7 V. Five thin film electrodes of each type were characterized by cyclic voltammetry.

2.5. Estimation of oxygen overpotentials

To compare the catalytic effects of the coprecipitated films on the OER, the overpotential at 10 mA was estimated from the voltammograms. For this, it was assumed that the return sweep provided the best approximation of the steady-state condition since there would be less interference from the nickel hydroxide redox reaction. Thus, the overpotential was

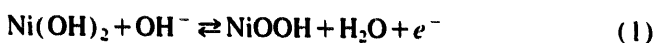
taken as the potential on the return sweep required to produce 10 mA of anodic current minus the reversible oxygen potential (taken as 303 mV versus Hg/HgO) [19].

3. Results and discussion

3.1. Precipitated films of single metal hydroxide

3.1.1. $\text{Ni}(\text{OH})_2$ electrode

The electrochemical behaviour of the S/ $\text{Ni}(\text{OH})_2$ electrode (S = Pt, C, Au, Ni) has been thoroughly investigated [20,21]. A voltammogram for $\text{Ni}(\text{OH})_2$ on a nickel substrate in 5 M KOH solution is shown in Fig. 1. The two current peaks, at 487 and 395 mV, correspond to the anodic and cathodic peaks of $\text{Ni}(\text{OH})_2$, respectively. The overall electrode reaction can be described as



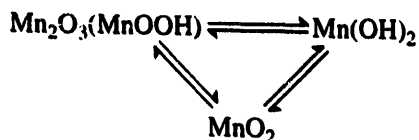
The current peak at 616 mV in Fig. 1 is due to oxygen evolution. The corresponding reaction is the discharge process of OH^-



3.1.2. $\text{Mn}(\text{OH})_2$ electrode

The cyclic voltammetry response of the $\text{Mn}(\text{OH})_2$ electrode is more complex than that of other electrodes due to a considerable loss of charge during potential cycling, as shown in Fig. 2.

According to the thermodynamic results obtained by Cordoba et al. [22] three cathodic peaks and three anodic peaks can be seen in the cyclic voltammogram for a Pt/ $\text{Mn}(\text{OH})_2$ electrode. The peaks correspond to the transition



The corresponding reaction equations are:

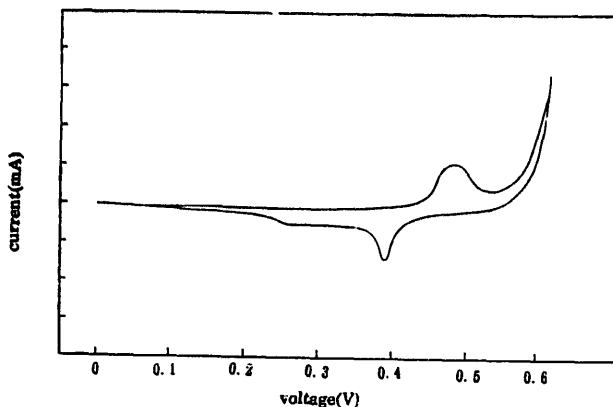
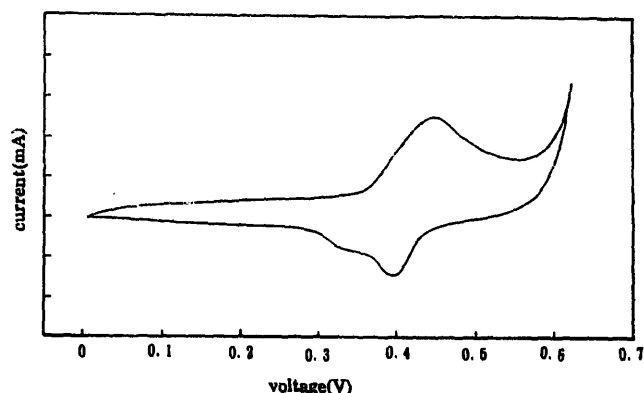
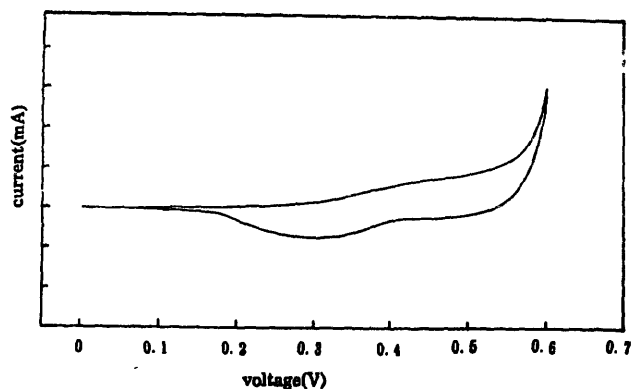
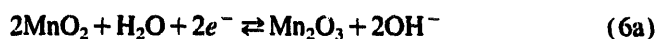
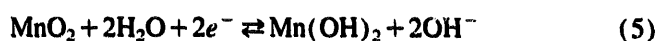


Fig. 1. Voltammogram for electrochemically precipitated $\text{Ni}(\text{OH})_2$.

Fig. 2. Voltammogram for electrochemically precipitated Mn(OH)₂.Fig. 3. Voltammogram for electrochemically precipitated Co(OH)₂.

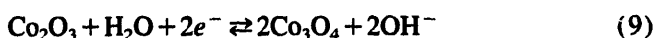
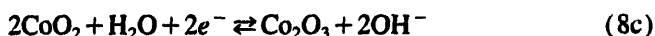
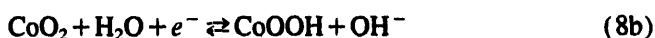
or



The same cyclic voltammetry response can be obtained for a Ni/Mn(OH)₂ electrode, except for the different peak potentials because different substrates and different precipitated conditions lead to different S/Mn(OH)₂ interfaces.

3.1.3. Co(OH)₂ electrode

Gosmez Meier et al. [23] have made a thorough investigation of the electrochemical behaviour in S/colloidal Co(OH)₂. Additionally, there have been many studies on oxide films grown on cobalt metal in alkaline solution. Cordoba et al. [22] examined the potential/dynamic response on the Pt/Co(OH)₂ electrode surface, and observed two anodic peaks during the initial sweep. Both peaks shifted towards a negative potential and the peak current decreased markedly from the second cycle. Moreover, a third peak appeared near the oxygen evolution potential. The three peaks correspond to the following reactions [18]:



The excess of anodic charge during the initial positive-going sweep is probably due to the formation of a species that is difficult to reduce. The potential range overlaps in the experiments reported here. Therefore, the peaks corresponding to the gain/loss of electrons cannot be distinguished clearly from each other (Fig. 3).

3.2. Cyclic voltammetry of binary coprecipitated films

The mixed nitrate deposition solutions have 0.05 M total metal concentration which consists of three parts of

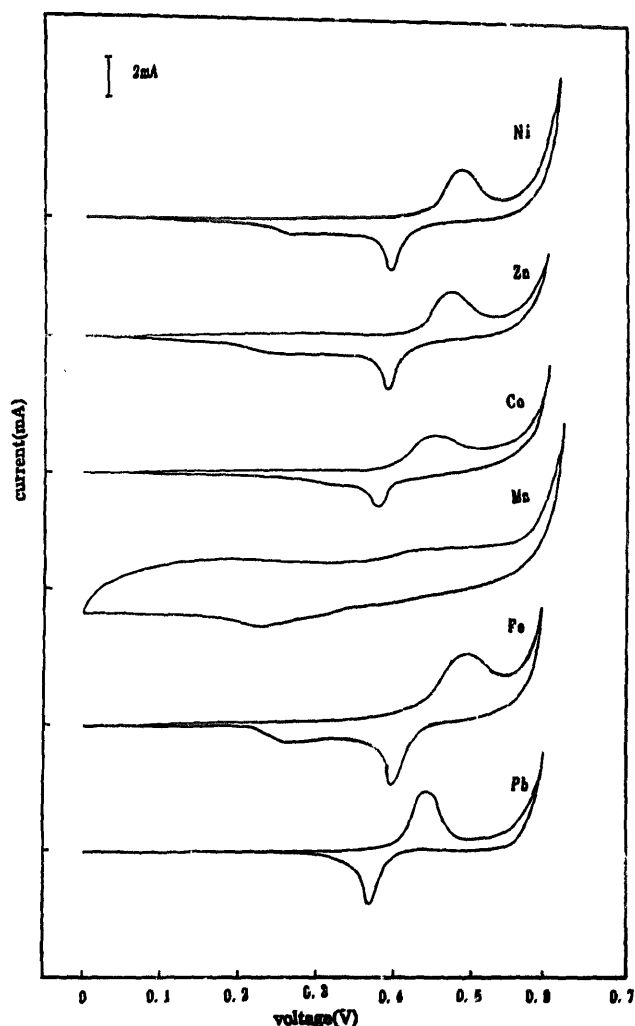


Fig. 4. Voltammogram for composite hydroxides with coprecipitated zinc, cobalt, manganese, iron and lead in 5 M KOH electrolyte.

Ni(NO₃)₂ solution and one part of one of Co(NO₃)₂, Mn(NO₃)₂, Zn(NO₃)₂, Fe(NO₃)₃ or Pb(NO₃)₂ solution (volume ratio).

Cyclic voltammograms for these coprecipitated films are shown in Fig. 4. The data show that the coprecipitation of these metal ions into Ni(OH)₂ thin films exerts some effects on the redox peaks of Ni(OH)₂ and the OER. These effects include change of peak position, catalysis or poisoning of oxygen evolution.

Table 1
Overpotentials for the OER on various coprecipitated thin films

Coprecipitated metal	OER overpotential (mV)
Ni ^a	313
Co	316
Mn	333
Zn	317
Fe	305
Pb	311

^a Ni(OH)₂ precipitated thin films.

3.2.1. Effect of coprecipitated hydroxides thin films on the overpotential for OER

The OER overpotentials of coprecipitated hydroxides thin films of various metals are shown in Table 1. The presence of cobalt, manganese or zinc increases the overpotential for OER. Manganese, in particular, exhibits a marked effect by increasing the OER overpotential by 20 mV. By contrast, the existence of lead or iron decreases the OER overpotential. The order of the effect of the various metals is: Mn > Zn > Co > Ni > Pb > Fe.

At more positive anodic potentials, oxygen gas is evolved according to



The current for the OER on a Ni(OH)₂ thin film is higher, that is, the overpotential for the OER is lower. The presence of coprecipitated metal alters the kinetics of the above reaction and, therefore, alters the overpotentials for the OER. According to the results obtained by Corrigan [18], coprecipitated cobalt can decrease the overpotential for OER, this is contrary to the results presented here. The difference may be related to the various coprecipitated conditions, such as current density, time, the content of metal.

3.2.2. Effect on peak potentials

The effect of coprecipitated metal on the redox peak potentials of Ni(OH)₂ are shown in Table 2. The effects on coprecipitated thin films electrodes are relatively weak, and the average peak potential is more negative except iron. Since the separation of the peak potentials and the average peak potential can act as a measure of reaction reversibility, coprecipitated metals improve the reversibility of Ni/Ni(OH)₂ by making the change from Ni(II) to Ni(III) more reversible.

Table 2
Redox peak potentials of Ni(OH)₂ at coprecipitated thin films

Coprecipitated metal	Anodic peak potential, E_a (mV)	Cathodic peak potential, E_c (mV)	Peak potential separation, ΔE (mV)	Average peak potential, \bar{E} (mV)
Ni	487	395	92	441
Zn	482	398	84	440
Co	472	393	79	432.5
Mn	446	380	66	413
Fe	490	398	82	444
Pb	459	386	73	423

Table 3
Overpotential for the OER at triplex coprecipitated thin films

Composition	OER overpotential (mV)
I	330
II	349
III	326
IV	318

The coprecipitated metals shift the peak potential to more positive values in the order Mn > Fe > Pb > Co > Zn > Ni.

3.3. Cyclic voltammetry of triplex coprecipitated thin films

The deposition solution consisted of Ni(NO₃)₂ and two of the other nitrate solutions; the total metal concentration was 0.05 M. The composition of the mixed solutions was:

- I. 8Ni + 1Co + 1Zn
- II. 8Ni + 1Mn + 1Zn
- III. 8Ni + 1Co + 1Pb
- IV. 8Ni + 1Co + 1Fe

The overpotentials for the OER are listed in Table 3. Clearly, all of the mixed solutions can increase the overpotential of the OER. The addition of cobalt inhibits the decline of the overpotential of the OER caused by the presence of iron or lead. The redox peak potentials are given in Table 4. It can be seen that the separation of the redox peak potentials for triplex coprecipitated thin films is smaller than that for Ni/Ni(OH)₂ thin films Fig. 5.

3.4. Ni(OH)₂ + Co(OH)₂ electrode

It can be seen from Tables 5 and 6 that both anodic and cathodic peak potentials shift to negative potentials with increase in the content of cobalt. This is because nickel and cobalt hydroxides form a solid solution and the lattice parameters change continuously with the composition of solid solution [24].

The shift of the anodic peak potential in a negative direction and the increase of the overpotential for OER are beneficial to the charge efficiency of Ni(OH)₂ electrode. The former is also beneficial in inhibiting the self-discharge of the Ni(OH)₂ electrode.

The potential/current response of Ni(OH)₂ and Co(OH)₂ coprecipitated in a proportion less than 50% has been studied

Table 4
Peak potentials of Ni(OH)₂ at triplex coprecipitated thin films

Composition	Anodic peak potential, E_a (mV)	Cathodic peak potential, E_c (mV)	Peak potential separation, ΔE (mV)	Average peak potential, \bar{E} (mV)
I	461	390	71	425.5
I'	381	329	52	355
III	431	360	71	395
IV	487	403	84	445

Table 5
Peak potentials of Ni(OH)₂ + Co(OH)₂ electrodes

Content of cobalt (wt.%)	Anodic peak potential, E_a (mV)	Cathodic peak potential, E_c (mV)	Peak potential separation, ΔE (mV)	Average peak potential, \bar{E} (mV)
0	487	395	92	441
25	472	393	79	432.5
50	424	338	86	381
75	436	318	118	377

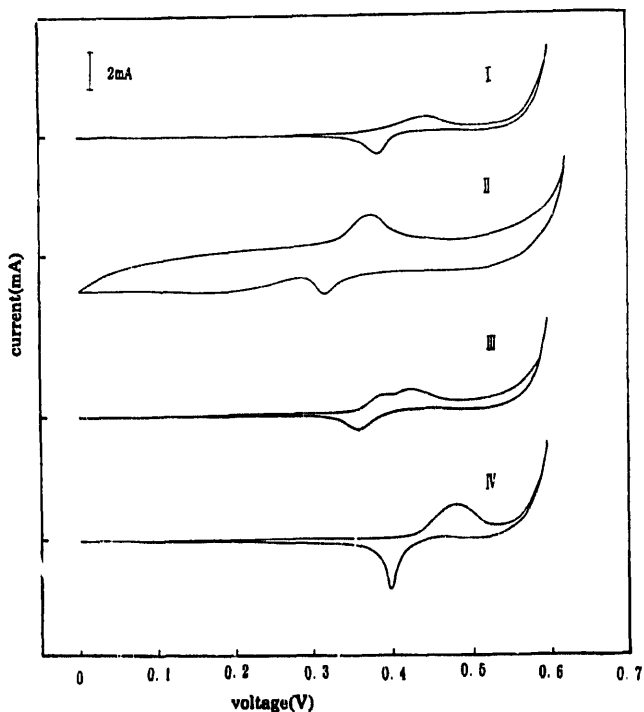


Fig. 5. Voltammogram for triplex coprecipitated metal hydroxides in 5 M KOH electrolyte.

by Folquer et al. [17]. It was concluded that the catalytic effects of the Co(II)/Co(III) reaction increases the reversibility of Ni(II)/Ni(III) reaction.

Cordoba et al. [22] found that, in the cyclic voltammetry of chemical coprecipitated Ni(OH)₂ and Co(OH)₂ thin films in a 1:1 ratio, the anodic peak displays a noticeable splitting into a minor and a major component during the first cycle, but from the second potential sweep onwards, the anodic peaks develop into a broad single peak.

Table 6
Overpotential for the OER on Ni(OH)₂ + Co(OH)₂ electrodes

Content of cobalt (wt.%)	OER overpotential (mV)
0	313
25	316
50	316
75	317
100	318

Armstrong [2] has investigated electrochemically coprecipitated Ni(OH)₂ and Co(OH)₂ thin films and found that when the content of cobalt is in the range of 25–75 wt.%, the anodic and cathodic peaks split into two peaks at rather slow sweep speeds, the separation of anodic/cathodic peak potentials increases with increase in the content of cobalt, and the overpotential for OER increase. Furthermore, the measurement of capacity shows that a two-electron process occurs in the redox reaction of Ni(OH)₂ [2].

3.5. Ni(OH)₂ + Mn(OH)₂ electrode

Cordoba et al. [22] consider that the Ni(OH)₂ + Mn(OH)₂ mixed phase is the most promising electrode for the OER in alkaline solution. Nevertheless, the nature of the interaction between the two phases and their subsequent effects are not clear. Accordingly, a study using cyclic voltammetry has been conducted in this work.

The coprecipitated manganese can affect the redox peak potentials and the overpotential for OER at the Ni(OH)₂ electrode. The effects are shown in Tables 7 and 8, respectively.

The existence of manganese causes the redox peak potentials of the Ni(OH)₂ electrode to shift in a negative direction.

Table 7
Peak potentials at Ni(OH)₂ + Mn(OH)₂ electrodes

Content of manganese (wt.%)	Anodic peak potential, E _a (mV)	Cathodic peak potential, E _c (mV)	Peak potential separation, ΔE (mV)	Average peak potential, \bar{E} (mV)
0	487	395	92	441
25	446	380	66	413
50	406	356	50	381
75	381	325	56	353
100	436	337	99	386.5

Table 8
Overpotential for the OER on Ni(OH)₂ + Mn(OH)₂ electrodes

Content of manganese (wt.%)	OER overpotential (mV)
0	313
25	333
50	351
75	352
100	354

When the content of manganese is 25–75 wt.%, the peak potentials become more negative with increase in the manganese content. This is in agreement with that at chemically coprecipitated thin films [22]. In the meantime, within the whole composition range, (i.e. 100 wt.%), the overpotential for OER increases with increase in the manganese content, and is higher than in the absence of manganese.

On the basis of the above results, the coprecipitated cobalt and manganese have the same influence on the redox peak potentials in shifting them towards negative potentials, and both increase the overpotential for the OER. The effects of manganese are more remarkable. Therefore, it seems that manganese can take the place of expensive cobalt in order to improve the electrode capacity and decrease the self-discharge in batteries.

3.6. Ni(OH)₂ + Zn(OH)₂ electrode

The effects of coprecipitated zinc on the redox peak potentials of Ni(OH)₂ and the overpotential for the OER are listed in Tables 9 and 10, respectively. It can be seen that the presence of zinc causes the redox peak potentials to shift towards

Table 9
Peak potentials at Ni(OH)₂ + Zn(OH)₂ electrodes

Content of zinc (wt.%)	Anodic peak potential, E _a (mV)	Cathodic peak potential, E _c (mV)	Average peak potential, \bar{E} (mV)	Peak potential separation, ΔE (mV)
0	487	395	441	92
25	482	398	440	84
50	472	393	432.5	79
75	477	393	435	86
100	479	396	437.5	83

negative values, but its effects are relatively unremarkable. When the content of zinc is 50 wt.%, the oxidation peak potential shifts by 15 mV, and the reduction peak potential shifts by only 2 mV. The coprecipitated zinc exerts the same effects as coprecipitated cobalt and manganese, namely, it increases the overpotential for the OER.

3.7. Ni(OH)₂ + Fe(OH)₃ electrode

The effects of coprecipitated iron on the redox peak potentials and the overpotential for the OER at Ni(OH)₂ electrode are presented in Tables 11 and 12, respectively. The redox peak potentials decrease dramatically and the overpotential for the OER decreases drastically with increasing iron content.

The results of Mlynarek et al. [25] showed that coprecipitated iron at the Ni(OH)₂ electrode results in an abrupt decrease of discharge capacity and overpotential, that is to say, iron exerts poisonous effects on the Ni(OH)₂ electrode. This conclusion is consistent with the findings presented here.

Two interpretations of the mechanism by which iron impurity modifies the electrochemical behaviour of the nickel hydroxide electrode are now explored. One interpretation is a multi-step mechanism [26,27]. The other explanation points out that the electrical resistance of nickel hydroxide of high valency affects the overpotentials for the OER [28,29], which is called a 'barrier layer effect', and it has been postulated that a highly resistive quadrivalent nickel hydroxide may result in high anodic potentials.

The deleterious effects of iron on nickel hydroxide electrodes are well known [30,31]. Voltammetric studies show that iron has a direct effect on the charge storage reactions. The anodic shifts and the increase of reversibility decrease

Table 10
Overpotentials for the OER on Ni(OH)₂ + Zn(OH)₂ electrodes

Content of zinc (wt.%)	OER overpotential (mV)
0	313
25	317
50	324
75	321
100	318

the transformation of α -phase nickel hydroxide to β -phase nickel hydroxide [32,33]. It is also likely that the conductivity of active material is affected. The main effects on the charge storage reaction appear to be catalysis of the OER which is parasitic to the charge process and thus exerts detrimental effects on the charge storage efficiency.

The addition of cobalt can inhibit the above deleterious effects. Armstrong et al. [34] and Corrigan [18] have investigated Ni(OH)₂-containing cobalt in KOH solution saturated with iron. The results show that the presence of cobalt inhibits the decrease in capacity due to the presence of iron. In the experiments reported here, a triplex coprecipitated thin film of nickel, cobalt and iron has been investigated and it is found that the presence of cobalt inhibits the shift of Ni(OH)₂ redox peak potentials towards negative values and the decrease of the overpotential for the OER (Tables 3 and 4). These results demonstrate that cobalt can act as an antidote to iron poisoning.

Nickel electrodes are the most common anodes used for alkaline water electrolysis. However, the high oxygen overpotential at these electrodes lowers the electrical efficiency [35]. To ameliorate this problem, considerable work has been done to develop electrocatalysts for the OER [36], and it is found that a composite of hydroxides of iron and nickel is a promising catalysts.

3.8. Ni(OH)₂ + Pb(OH)₂ electrode

The effects of coprecipitated lead in Ni(OH)₂ on redox peak potentials and the overpotential for the OER are listed in Tables 13 and 14, respectively. The data show that when the content of lead falls in the range 0–75 wt.%, the redox peak potentials of Ni(OH)₂ and the overpotential for the OER decrease with increase in the content of lead. The presence

Table 12
Overpotentials for the OER on Ni(OH)₂ + Fe(OH)₃ electrodes

Content of iron (wt.%)	OER overpotential (mV)
0	313
25	305
50	302
75	302
100	311

of lead leads to a decrease in the overpotential for the OER on the Ni(OH)₂ electrode and, therefore, the charge efficiency decreases, which is considered to be harmful to batteries.

The data in Tables 3 and 4 show that the deleterious effect of lead on the Ni(OH)₂ electrode might be inhibited by adding cobalt. The latter not only causes the redox peak potentials to shift towards negative values, but also increases markedly the overpotential for the OER. Thus, the charge efficiency can be improved significantly.

4. Conclusions

The effects of cobalt, manganese, zinc, lead and iron on the cyclic voltammetry behaviour of electrochemically coprecipitated Ni(OH)₂ electrode are examined. Experiments indicate that the addition of cobalt, manganese and zinc increases the overpotential for the OER at the Ni(OH)₂ electrode, and decreases the redox peak potentials of Ni(OH)₂. This is beneficial to nickel electrodes when used in batteries, because their charge efficiency can be improved while the addition of lead or iron decreases the overpotential of the OER on Ni(OH)₂ electrodes. The coprecipitated iron causes the redox peak potentials to shift towards positive potentials. Therefore, iron and lead are usually thought to be deleterious to nickel electrodes used in batteries. The addition of iron decreases the overpotential for the OER significantly, which is beneficial to the electrolysis of alkaline aqueous solution, because the current efficiency might be increased. The deleterious effects of iron and lead can be inhibited by the addition of cobalt.

Table 11
Peak potentials at Ni(OH)₂ + Fe(OH)₃ electrodes

Content of iron (wt.%)	Anodic peak potential, E_a (mV)	Cathodic peak potential, E_c (mV)	Average peak potential, \bar{E} (mV)	Peak potential separation, ΔE (mV)
0	487	395	441	92
25	490	398	444	92
50	492	400	446	92
75	495	405	450	90
100	487	395	441	92

Table 13
Peak potentials at Ni(OH)₂ + Pb(OH)₂ electrodes

Content of lead (wt.%)	Anodic peak potential, E _a (mV)	Cathodic peak potential, E _c (mV)	Average peak potential, \bar{E} (mV)	Peak potential separation, ΔE (mV)
0	487	395	441	92
25	459	386	422.5	73
50	454	386	320	68
75	446	380	413	66
100	462	396	429	66

Table 14
Overpotentials for the OER on Ni(OH)₂ + Pb(OH)₂ electrodes

Content of lead (wt.%)	OER overpotential (mV)
0	313
25	311
50	310
75	307
100	324

References

- [1] M. Oshitani, H. Yufu, K. Takashima, S. Tsuji and Y. Matsumaru, *J. Electrochem. Soc.*, **136** (1989) 1590.
- [2] R.D. Armstrong, *J. Power Sources*, **25** (1989) 89.
- [3] S.U. Falk and A.J. Salkind, *Alkaline Storage Batteries*, Wiley, New York, 1969.
- [4] S. Jannskiewicz, *Proc. 13th Annual Power Sources Conf., 1959*, p. 75.
- [5] D.H. Fritts, *J. Electrochem. Soc.*, **129** (1982) 118.
- [6] W. Lee, *J. Electrochem. Soc.*, **132** (1985) 2835.
- [7] B. Klaspste, K. Micka, J. Mrha and J. Vondrak, *J. Power Sources*, to be published.
- [8] E.J. Casey, A.R. Dubois, P.E. Lake and W.J. Moroz, *J. Electrochem. Soc.*, **112** (1965) 371.
- [9] M. Oshitani, Y. Sasaki and K. Takashima, *J. Power Sources*, **12** (1984) 219.
- [10] M. Oshitani, T. Takashima and S. Tsuji, *J. Appl. Electrochem.*, **16** (1986) 403.
- [11] A. Hekling and S. Hill, *Discuss. Faraday Soc.*, **1** (1947) 236.
- [12] S. Trasatti and G. Lodi, *Electrodes of Conductive Metallic Oxides*, 1981, p. 521.
- [13] M.H. Miles, *J. Electroanal. Chem.*, **60** (1975) 89.
- [14] S. Trasatti, *Electrochim. Acta*, **29** (1984) 1503.
- [15] H. Dieng, O. Contamin and M. Savy, *J. Electrochem. Soc.*, **125** (1978) 1026.
- [16] D.F. Pickett and J.T. Maloy, *J. Electroanal. Chem.*, **172** (1984) 235.
- [17] M.E. Folquer, J.R. Vilche and A.J. Arvia, *J. Electroanal. Chem.*, **172** (1984) 235.
- [18] D.A. Corrigan, *J. Electrochem. Soc.*, **134** (1987) 377.
- [19] J.G. Ives and G.J. Janz, *Reference Electrodes Theory and Practice*, Academic Press, New York, 1961.
- [20] R.E. Carbonio, V.A. Macagno, M.C. Giodano, J.R. Vilche and A.J. Arvia, *J. Electrochem. Soc.*, **129** (1982) 983.
- [21] R.E. Carbonio, V.A. Macagno and A.J. Arvia, *J. Electrochem. Soc.*, **129** (1982) 983.
- [22] S.I. Cortoba, R.E. Carbonio, M. Lopez and V.A. Macagno, *Electrochim. Acta*, **31** (1986) 1321.
- [23] H. Gomez Meier, J.R. Vilche and A.J. Arvia, *J. Electroanal. Chem.*, **134** (1982) 251; **138** (1982) 367.
- [24] W.D. Johnson, R.C. Miller and R. Mazelsky, *J. Phys. Chem.*, **172** (1984) 235.
- [25] G. Mlynarek, M. Paszkiewicz and A. Radniecks, *J. Appl. Electrochem.*, **14** (1984) 145.
- [26] J.O'M. Bockeric, *J. Chem. Phys.*, **24** (1956) 817.
- [27] A.C. Riddiford, *Electrochim. Acta.*, **4** (1961) 170.
- [28] P.W.T. Lu and S. Srinivasan, *J. Electrochem. Soc.*, **125** (1978) 1631.
- [29] R.E. Mayer, *J. Electrochem. Soc.*, **107** (1960) 847.
- [30] R.L. Tichener, *Ind. Eng. Chem.*, **44** (1952) 973.
- [31] M.Z.A. Munshi, A.C.C. Tsung and J. Parker, *J. Appl. Electrochem.*, **15** (1985) 711.
- [32] P. Oliva, *J. Power Sources*, **8** (1982) 229.
- [33] D.M. MacArthur, *J. Electrochem. Soc.*, **117** (1970) 422.
- [34] R.D. Armstrong, G.W.D. Briggs and E.A. Charles, *J. Appl. Electrochem. Soc.*, **18** (1988) 215.
- [35] D.E. Hall, *J. Electrochem. Soc.*, **132** (1985) 41C.
- [36] J. Orehotsky, H. Huang, C.R. Davidson and Srinivasan, *J. Electroanal. Chem.*, **95** (1978) 233.